Grain size, mineralogical and geochemical studies of coastal and inland dune sands from El Vizcaíno Desert, Baja California Peninsula, Mexico

Juan José Kasper-Zubillaga[1,*] and Hugo Zolezzi-Ruiz[2]

[1] Instituto de Ciencias del Mar y Limnología, Geología Marina y Ambiental, Universidad Nacional Autónoma de México, Circuito Exterior s/n, 04510, México D.F., Mexico.
[2] Posgrado en Ciencias del Mar y Limnología, Instituto de Ciencias del Mar y Limnología, Universidad Nacional Autónoma de México, Circuito Exterior s/n, 04510, México D.F. , Mexico.
** kasper@icmyl.unam.mx*

ABSTRACT

A sedimentological, petrological and geochemical research work was carried out in order to find out the origin and provenance of coastal and inland desert dunes from El Vizcaíno Desert, northwestern Mexico. Fifty four sand samples were collected from the windward, crest and slip face of coastal and desert dunes (barchan, transverse, aeolian sand sheets). Onshore winds generates fine, well sorted, near symmetrical dune sands with mesokurtic distributions in the El Vizcaíno Desert inherited from beach sands from the Vizcaíno bay. The coastal and inland dune sands are derived from nearby sand sources like the beach sands and also from alluvial deposits originated from sedimentary-volcanic and schists, granitic and granodiorite sources. This is evidenced by the presence of high quartz content, shell debris, carbonates, mica and hornblende that are constituents of the both coastal and inland dune sands and are probably derived from the action of longshore drifts and onshore winds. The El Vizcaíno coastal and inland dune sands are placed in the craton interior and recycled orogen fields in the Q-F-L diagram suggesting intrusive, sedimentary and partly metamorphosed sources in the composition of the sand. The geochemistry of the sands supports also the maturity process of the sands mainly associated with the presence of alluvial deposits and marine-aeolian action. Additionally, the El Vizcaíno dune sands are chemically related to acid rocks, felsic-plutonic detritus source rocks, which are associated to an active continental margin. The low chemical index of alteration (CIA) values in the dune sands suggest that dryness of the area plays a role in the preservation of labile minerals. The presence of volcanic, metamorphic and plutonic rock around the El Vizcaíno desert basin might contribute to the higher content of plagioclase and mica in the sands when compared to other North American deserts.

Key words: grain size, mineralogy, geochemistry, provenance, coastal and inland dune sands, Vizcaíno Desert, Mexico.

RESUMEN

Se realizó un estudio sedimentológico, petrológico y geoquímico en arena de dunas para establecer el origen y procedencia de las dunas costeras y continentales del Desierto de El Vizcaíno, Noroeste de México. Cincuenta y cuatro muestras se colectaron del barlovento, cresta y sotavento de dunas costeras y continentales (barjan, transversales, depósitos eólicos arenosos). Vientos hacia la costa generan arenas finas, bien clasificadas, casi simétricas, con distribuciones mesocúrticas en el Desierto de El Vizcaíno heredadas de la arena de playa de la Bahía del Vizcaíno. Las dunas costeras y continentales se derivan de fuentes cercanas como las playas, pero también de depósitos aluviales originados a partir de rocas sedimentarias, volcánicas y esquistos, graníticas y granodioritas. La evidencia está en la presencia de fragmentos de conchas, carbonatos, mica y hornblenda que componen las dunas costeras y continentales y que se derivan por transporte litoral y vientos hacia la costa. Las dunas costeras y continentales del

Vizcaíno se clasifican dentro del cratón interior y orógeno reciclado en el diagrama C-F-L sugiriendo fuentes intrusivas, sedimentarias y parcialmente metamorfoseadas en la composición de la arena. La geoquímica respalda el proceso de madurez composicional de la arena de duna asociada a la presencia de depósitos aluviales y acción marina-eólica. Adicionalmente, las dunas del Vizcaíno están químicamente relacionadas a rocas ácidas, fuentes félsicas-plutónicas asociadas a una margen continental activa. El bajo índice de alteración química (IAQ) en las dunas indica que el clima seco del área juega un papel importante en la preservación de minerales inestables. La presencia de rocas volcánicas, metamórficas y plutónicas alrededor del Vizcaíno contribuye a la presencia de plagioclasa y mica en comparación con otros desiertos de Norteamérica.

Palabras clave: tamaño de grano, mineralogía, geoquímica, procedencia, dunas costeras y continentales, Desierto de El Vizcaíno, México.

INTRODUCTION

Coastal and inland dune sands in desert environments are compositionally and texturally controlled by physical and chemical processes such as the wind action, marine/ fluvial processes, weathering, air temperature and precipitation (Pye and Mazzullo, 1994; Lancaster 1995; Livingstone *et al.,* 1999; Muhs and Holliday, 2001; Garzanti *et al.,* 2003; Muhs *et al.*, 2003, Honda *et al.*, 2004). Grain size variations in coastal and desert dune sands have been widely used to infer transport and depositional mechanisms (Bagnold, 1941; Khalaf, 1989, Pye and Tsoar, 1990; Lancaster, 1992; Wang *et al.*, 2003; Kasper-Zubillaga and Carranza-Edwards, 2005). For example, size coarsening of the dune sands may be due to wind deflation of fine grains leaving behind the coarse fraction in the sands (Khalaf, 1989). It has been also observed that moderately to poorly sorted dune sands occur with short transport from the source of sediments to the dune systems (Blount and Lancaster, 1990). In contrast, longer aeolian transport produces better sorted and fine-grained dune sands (Leeder, 1982; Kasper-Zubillaga and Carranza Edwards 2005). In addition, mineralogical and geochemical studies of dune sands provide new insights into the origin and evolution of aeolian sand bodies (Muhs, 2004). Quartz-rich sand dunes are mineralogically mature and they might have inherited their composition from quartz-rich sandstones and weathered plutonic and metamorphic rocks. Maturity of the sands might also be related to losses of labile minerals like feldspar grains due to ballistic impacts in high energy aeolian environments, chemical weathering of feldspar in soils, and fluvial size reduction of feldspars (Dutta *et al.*, 1993; Muhs *et al.*, 2003; Muhs 2004). In contrast, feldspar-rich dune sands might be derived from feldspar-rich sources (arkosic sources) but also by little chemical weathering and short aeolian transport (Muhs, 2004).

In this paper, we establish the provenance of coastal and inland dune sands from El Vizcaíno Desert, Baja California Peninsula, Mexico. The specific aim of this paper is to observe the grain size attributes, mineralogical and geochemical differences between the dune fields close to the beaches of the Vizcaíno Bay and the inland dune fields to interpret the processes (*i.e.*, fluvial, aeolian, chemical) that dominate the grain size characteristics and composition of both dune fields. Furthermore, this study provides information on dune sands probably derived from a mix of sedimentary, volcanic, metamorphic and plutonic rocks. Our hypothesis states that the El Vizcaíno dune sands are probably influenced by more than one source rock compared to other North American desert dunes (*i.e.*, Altar Desert, Mexico, Algodones Dunes, California, and Parker Dunes, Arizona) (Muhs *et al.,* 1995; Winspear and Pye, 1995; Zimbelman and Williams, 2002; Muhs *et al.,* 2003; Kasper-Zubillaga *et al.*, 2006b, in press) but still with mature composition despite the complex lithology surrounding the dune fields.

STUDY AREA

The study area is located in the Baja California Peninsula, Mexico between 26º 29' and 28º 30' N and 112º 15' 45" and 115º 15' W. (Figure 1a). The low elevations of the central and western parts of the reserve receive constant coastal winds and intense solar radiation. Altitudes range from 0 m at the coast to 1,985 m above sea level at the highest peaks in the mountains.

According to Köeppen (1948), climate in the El Vizcaíno Desert is arid (Bw) with an average annual rainfall between 10 to 25 mm (Tamayo, 2000). Onshore winds are northerly, westerly and northwesterly measured at the Vizcaíno Bay (Pérez-Villegas, 1989). Northerly and westerly winds occur 10 % to 30 % of the time in one month with velocities between 2 to 4 $m \cdot s^{-1}$, whilst northwesterly winds occur 40 % of the time in one month with velocities between 4 to 6 $m \cdot s^{-1}$ (Pérez-Villegas, 1989). Longshore current comes from the north with average velocities from 6 to 12 $cm \cdot s^{-1}$ (Fernández-Eguiarte *et al.,* 1992). Average wave height is 2.4 m near Guerrero Negro and further north (Buoy Weather, 2005). The geomorphological unit in the western coastal area of the Baja California Peninsula is the Western Californian Plain (WCP) (Tamayo, 2000). Average slope in Guerrero Negro and northern beaches is

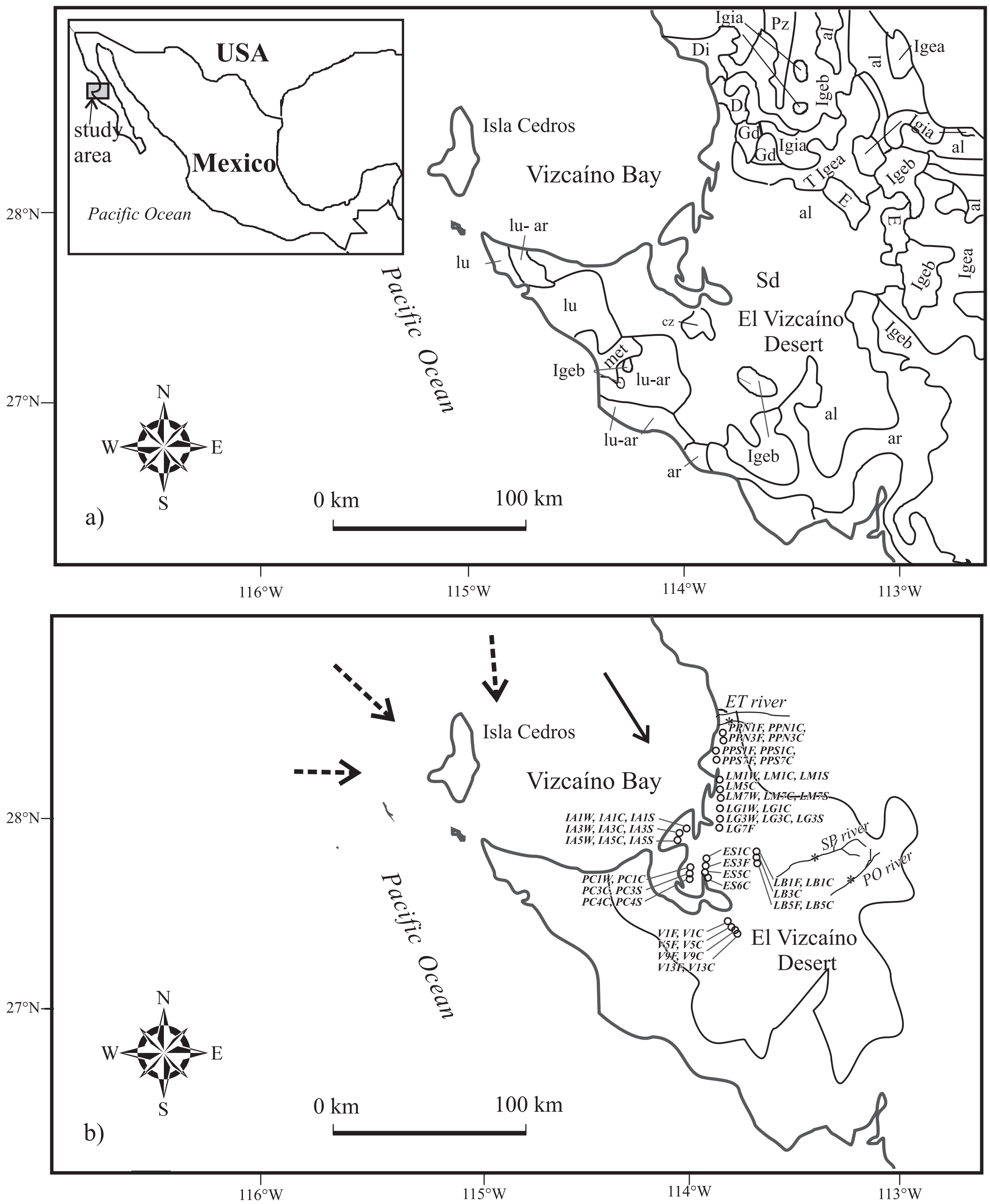

Figure 1. a) Simplified geological map of the studied and surrounding areas (Padilla y Sánchez and Aceves-Quesada, 1992). Sedimentary rocks: lu : shale; ar: sandstone; cg: conglomerate; cz: limestone; al: alluvial; Sd: sand dunes. Metamorphic rocks: pz: slate; E: schist; met: metamorfic complex. Extrusive igneous rocks: Igea: acid; Igeb: basic. Intrusive igneous rocks: Igia: acid; Di; diorite; Gd: granodiorite; cbu: ultrabasic complex. b) Sampling sites of the study area. See Table 1 for sampling keys and coordinates. Asterisks represent the fluvial sand sampling site. Arrow shows the prevail longshore drift and dotted arrows show the prevail onshore winds (Fernández-Eguiarte *et al.*, 1992; Pérez-Villegas, 1989). Rivers: ET: El Tomatal, SP: San Pablo, PO: El Porvenir.

4.3º (Carranza-Edwards *et al.*, 1998).

Coastal dunes are mobile and semimobile, vegetated dune types, and morphologically they are barchan, transverse and linear types. Desert dunes are vegetated, semimobile, linear and transverse dune types (Inman *et al.*, 1966; Zolezzi-Ruiz, 2007).

The El Vizcaíno Desert is surrounded by shales, sandstones, conglomerate, and limestones present mainly in the southern part of the desert basin. Slate and schists are also present in the north, and basalts, rhyolite, granites, diorites and granodiorites in the northern and the eastern part of the basin (Figure 1a).

MATERIALS AND METHODS

A systematic dune sand sampling was performed on coastal and inland dune sands during May-June 2005 (Figure 1b). Samples were collected from the windward, crest and slip face of coastal and desert barchan dunes and transverse sand sheets from El Vizcaíno Desert. This was done because in some cases such as in certain linear and crescent dunes, morphology might control the grain size parameters and mineralogy of the coastal (Kasper-Zubillaga and Dickinson, 2001) and desert dunes (Lancaster 1983; Watson; 1986; Livingstone *et al.*, 1999; Wang *et al.*, 2003). Fifty four sand samples were placed in plastic bags, labeled and separated for grain size, thin sectioning and geochemical determinations. A Global Positioning System (GPS) was used to locate sampling sites and to measure dune heights above sea level.

Approximately 1 to 2 g of sand samples were used for grain size analysis after storing 10 g of each sand sample to ensure repeatability in the grain size analysis. The grain size analysis was performed with a Laser Particle Size Analyser (Model Coulter LS230) that determines the particle sizes between –1.0 ϕ and 14.6 ϕ. Particle size distributions were given in μm and converted into ϕ units to calculate the grain size distribution parameters with the formula Log_2 (mm) and percentiles utilized in Folk´s formulae (Folk, 1980) (Table

Table 1. Grain size parameters of the coastal dune sands from the El Vizcaíno Desert (*n*= 41).

Location and sampling site	Mz	σ	Ski	K_G
1. Playa Pacheco Norte. Transverse dunes				
PPN1F 114º 03’; 28º 25’	2.596	0.397	0.069	0.990
PPN1C 114º 03’; 28º 25’	2.536	0.391	0.053	0.987
PPN3F 114º 04’; 28º 26’	2.561	0.391	0.061	0.985
PPN3C 114º 04’; 28º 26’	2.569	0.376	0.057	0.997
Average	2.566	0.389	0.060	0.990
Standard deviation	0.025	0.009	0.007	0.005
2. Playa Pacheco Sur. Transverse dunes				
PPS1F 114º 05’; 28º 18’	2.359	0.391	0.013	0.969
PPS1C 114º 05’; 28º 18’	2.314	0.400	0.007	0.965
PPS7F 114º 06’; 28º 19’	2.446	0.400	0.036	0.984
PPS7C 114º 06’; 28º 19’	2.483	0.405	0.052	1.005
Average	2.401	0.399	0.027	0.981
Standard deviation	0.078	0.006	0.021	0.018
3. Laguna Manuela. Batchan Dunes				
LM1W 114º 02’; 28º 13’	2.486	0.436	-0.039	1.029
LM1C 114º 02’; 28º 13’	2.537	0.462	-0.024	1.016
LM1S 114º 02’; 28º 13’	2.407	0.432	-0.051	1.040
LM5C 114º 03’; 28º 12’	2.580	0.394	0.045	0.977
LM7W 114º 03’; 28º 12’	2.554	0.403	0.013	0.978
LM7C 114º 03’; 28º 12’	2.587	0.392	0.037	0.970
LM7S 114º 03’; 28º 12’	2.586	0.379	0.025	0.962
Average	2.534	0.414	0.001	0.996
4. La Golondrina. Barchan Dunes				
LG1W 114º 02’; 28º 07’	2.674	0.362	0.025	0.952
LG1C 114º 02’; 28º 07’	2.659	0.374	0.024	0.960
LG3W 114º 03’; 28º 06’	2.622	0.392	0.017	0.978
LG3C 114º 03’; 28º 06’	2.528	0.433	-0.024	1.009
LG3S 114º 03’; 28º 06’	2.533	0.397	-0.005	0.971
LG7F 114º 03’; 28º 06’	2.710	0.364	0.033	0.957
Average	2.621	0.387	0.012	0.971
Standard deviation	0.076	0.027	0.022	0.021
5. Isla de Arena. Barchan Dunes				
IA1W 114º 07’; 28º 02’	2.094	0.904	-0.455	0.991
IA1C 114º 07’; 28º 02’	2.451	0.543	-0.184	1.259
IA1S 114º 07’; 28º 02’	2.028	1.001	-0.491	0.847
IA3W 114º 08’; 28º 01’	2.403	0.636	-0.269	1.424
IA3C 114º 08’; 28º 01’	2.498	0.466	-0.089	1.084
IA3S 114º 08’; 28º 01’	2.593	0.400	-0.009	0.985
IA5W 114º 08’; 28º 01’	2.623	0.400	0.000	0.987
IA5C 114º 08’; 28º 01’	2.591	0.416	-0.025	1.006
IA5S 114º 08’; 28º 01’	2.619	0.397	-0.004	0.987
Sverage	2.433	0.574	-0.170	1.063
Standard deviation	0.225	0.230	0.195	0.174
6. Exportadora de Sal. Transverse dunes				
ES1F 114º 05’; 27º 55’	2.500	0.395	0.029	0.985
ES1C 114º 05’; 27º 55’	2.530	0.383	0.029	0.968
ES3F 114º 05’; 27º 54’	2.475	0.398	0.032	0.974
ES5F 114º 05’; 27º 54’	2.412	0.390	0.016	0.956
ES5C 114º 05’; 27º 54’	2.442	0.393	0.031	0.964
ES6C 114º 05’; 27º 54’	2.688	0.493	0.164	1.205
Average	2.508	0.409	0.050	1.009
Standard deviation	0.098	0.042	0.056	0.097
7. Puerto Chaparrito. Barchan Dunes				
PC1W 114º 07’; 27º55’	1.875	0.776	-0.240	0.936
PC1C 114º 07’; 27º 55’	2.281	0.555	-0.132	1.170
PC3C 114º 08’; 27º 54’	2.026	0.716	-0.222	1.147
PC3S 114º 08’; 27º 54’	2.251	0.515	-0.145	1.163
PC4C 114º 08’; 27º 54’	2.506	0.387	0.009	0.981
PC4S 114º 08’; 27º 54’	2.413	0.383	0.009	0.954
Average	2.225	0.555	-0.120	1.059
Standard deviation	0.237	0.164	0.108	0.112
8. El Vizcaíno. Transverse dunes				
V1F 113º 50’; 27º 30’	2.646	0.395	0.051	0.991
V1C 113º 50’; 27º 30’	2.702	0.399	0.067	0.984
V5F 113º 49’; 27º 29’	2.619	0.382	0.053	0.975
V5C 114º 49’; 28º 29’	2.632	0.392	0.037	0.984
V9F 114º 49’; 28º 29’	2.677	0.378	0.046	0.959
V9C 114º 49’; 28º 29’	2.632	0.413	0.047	1.000
V13F 114º 48’; 28º 28’	2.679	0.395	0.057	0.976
V13C 114º 48’; 28º 28’	2.743	0.404	0.072	0.993
Average	2.666	0.395	0.054	0.983
Standard deviation	0.042	0.011	0.011	0.013
9. La Bombita. Transverse dunes				
LB1F 113º 46’; 27º 53’	1.539	1.005	0.160	0.950
LB1C 113º 46’; 27º 53’	2.536	0.945	0.111	1.582
LB3C 113º 47’; 27º 52’	2.694	0.450	0.023	1.012
LB5F 113º 47’; 27º 52’	2.498	0.497	0.041	1.018
LB5C 113º 47’; 27º 52’	2.769	0.398	0.055	1.002
Average	2.407	0.659	0.078	1.113
Standard deviation	0.498	0.291	0.056	0.264

Mz: mean graphic size, σ: sorting, Ski: skewness, K_G: kurtosis. See text for formulae used to determine grain size parameters. F: dune flank, C: dune crest, W: windward, S: slip face. The data were not tested for possible outliers although suggested by Verma and Quiroz-Ruiz (2006).

1). Graphic mean represents the average grain size and it was calculated using Mz= (ϕ16 + ϕ50 + ϕ84)/3. Sorting represents the degree in which the sediment is mixed with coarse and fine sizes. It is computed with (ϕ84 - ϕ16)/4 + (ϕ95 - ϕ5)/6.6. Skewness is a measure of symmetry in a grain size distribution. Its values can be obtained with (ϕ16 + ϕ84 - 2ϕ50)/(ϕ84 - ϕ16). Kurtosis is the degree of peakedness in the graphic distribution (Folk, 1980).

Fifty four thin sections of bulk composition were prepared to analyze the dune sands. Point counting was carried out using the traditional standard method of 250 grains for the major compositional framework of quartz, feldspar and lithics in 54 dune sand samples and three river sand samples (Franzinelli and Potter 1983) (Tables 2 and 3). This was done because quartz enrichment of the sands and little dispersion in the size fractions has been observed in dune sands (Livingstone *et al.*, 1999; Wang *et al.*, 2003; Honda *et al.*, 2004; Muhs, 2004; Kasper-Zubillaga and Carranza-Edwards, 2005). Additionaly 50 grains were counted for minor components like opaque minerals (magnetite)(Op), translucid heavy minerals (pyroxenes, hornblende, apatite, ilmenite, magnetite)(Hm), mica (biotite, chlorite)(Mc) and

Table 2. Point counts of dune sands from the El Vizcaíno Desert.

Sample	Qm	Qp	Fk	P	Lv	Ls	Lm	Lp	Total	Op	Hm	Mc	Bg+C	Total	Qt (%)	Ft (%)	Lt (%)
Coastal dunes																	
PPN1F	194	2	0	22	11	10	6	5	250	7	2	40	1	50	78.4	8.8	12.8
PPN1C	192	8	3	23	9	8	4	3	250	8	1	36	5	50	80	10.4	9.6
PPN3F	201	2	1	26	4	12	2	2	250	6	1	42	1	50	81.2	10.8	8
PPN3C	210	4	3	12	5	12	2	2	250	6	5	38	1	50	85.6	6	8.4
Average	199	4	1.8	21	7.25	10.5	3.5	3	250	6.8	2.3	39	2	50	81.3	9.0	9.7
Standard deviation	8.14	2.83	1.50	6.08	3.30	1.91	1.91	1.41	0.00	0.96	1.89	2.58	2.00	0.00	3.09	2.18	2.18
PPS1F	201	2	3	19	10	12	2	1	250	8	0	36	6	50	81.2	8.8	10
PPS1C	214	0	1	16	6	9	1	3	250	0	4	35	11	50	85.6	6.8	7.6
PPS7F	190	7	0	23	7	18	3	2	250	3	2	37	8	50	78.8	9.2	12
PPS7C	198	5	0	22	6	16	1	2	250	3	4	34	9	50	81.2	8.8	10
Average	201	3.5	1	20	7.25	13.8	1.75	2	250	3.5	2.5	36	8.5	50	81.7	8.4	9.9
Standard deviation	9.98	3.11	1.41	3.16	1.89	4.03	0.96	0.82	0.00	3.32	1.91	1.29	2.08	0.00	2.84	1.08	1.80
LM1W	200	3	1	22	2	15	3	4	250	7	0	32	11	50	81.2	9.2	9.6
LM1C	196	3	2	17	7	21	0	4	250	6	2	21	21	50	79.6	7.6	12.8
LM1S	213	3	1	14	5	13	0	1	250	5	3	34	8	50	86.4	6	7.6
LM5C	201	6	0	17	5	19	0	2	250	8	4	32	6	50	82.8	6.8	10.4
LM7W	205	2	1	20	2	16	0	4	250	5	4	31	10	50	82.8	8.4	8.8
LM7C	197	7	0	25	4	12	1	4	250	5	4	34	7	50	81.6	10	8.4
LM7S	191	3	2	26	1	22	4	1	250	2	3	38	7	50	77.6	11.2	11.2
Average	200	3.86	1	20	3.71	16.9	1.14	2.9	250	5.4	2.9	32	10	50	81.7	8.5	9.8
Standard deviation	7.07	1.86	0.82	4.45	2.14	3.89	1.68	1.46	0.00	1.90	1.46	5.25	5.16	0.00	2.77	1.82	1.79
LG1W	195	7	0	18	4	23	2	1	250	5	0	33	12	50	80.8	7.2	12
LG1C	212	2	1	22	1	12	0	0	250	4	0	37	9	50	85.6	9.2	5.2
LG3W	198	4	1	22	2	19	1	3	250	13	2	27	8	50	80.8	9.2	10
LG3C	194	5	1	19	6	24	0	1	250	12	0	27	11	50	79.6	8	12.4
LG3S	215	4	1	15	2	10	1	2	250	5	1	34	10	50	87.6	6.4	6
LG7F	213	4	1	11	3	14	2	2	250	5	3	35	7	50	86.8	4.8	8.4
Average	205	4.33	0.8	18	3	17	1	1.5	250	7.3	1	32	9.5	50	83.5	7.5	9.0
Standard deviation	9.81	1.63	0.41	4.26	1.79	5.87	0.89	1.05	0.00	4.03	1.26	4.22	1.87	0.00	3.51	1.71	3.01
IA1W	190	18	1	20	2	14	0	5	250	0	0	5	45	50	83.2	8.4	8.4
IA1C	190	14	2	25	3	16	0	0	250	0	0	7	43	50	81.6	10.8	7.6
IA1S	199	11	0	17	4	15	3	1	250	2	0	4	44	50	84	6.8	9.2
IA3W	189	12	4	22	4	17	0	2	250	1	0	8	41	50	80.4	10.4	9.2
IA3C	192	15	0	21	7	13	2	0	250	1	1	7	41	50	82.8	8.4	8.8
IA3S	195	14	2	19	4	16	0	0	250	0	0	12	38	50	83.6	8.4	8
IA5W	197	13	0	21	3	14	2	0	250	3	0	6	41	50	84	8.4	7.6
IA5C	187	12	2	18	8	19	3	1	250	6	0	11	33	50	79.6	8	12.4
IA5S	183	18	0	26	6	15	1	1	250	4	1	11	34	50	80.4	10.4	9.2
Average	191	14.1	1.2	21	4.56	15.4	3	1.1	250	1.9	0.2	8	40	50	82.2	8.9	8.9
Standard deviation	5.02	2.52	1.39	3.00	2.01	1.81	1.30	1.62	0.00	2.09	0.44	2.85	4.21	0.00	1.71	1.34	1.46

Table 2. (Continued).

Sample	Qm	Qp	Fk	P	Lv	Ls	Lm	Lp	total	Op	Hm	Mc	Bg+C	total	Qt (%)	Ft (%)	Lt (%)
ES1C	189	4	1	23	6	22	2	3	250	4	1	28	17	50	77.2	9.6	13.2
ES3F	204	4	2	21	0	15	2	2	250	8	3	24	15	50	83.2	9.2	7.6
ES5F	214	4	0	16	2	11	1	2	250	2	1	20	27	50	87.2	6.4	6.4
ES5C	200	2	2	28	2	10	4	2	250	3	0	21	26	50	80.8	12	7.2
ES6C	213	2	0	22	3	8	2	0	250	15	0	25	10	50	86	8.8	5.2
Average	204	3.2	1	22	2.6	13.2	2.2	1.8	250	6.4	1	24	19	50	82.9	9.2	7.9
Standard deviation	10.27	1.10	1.00	4.30	2.19	5.54	1.10	1.10	0.00	5.32	1.22	3.21	7.31	0.00	4.03	2.00	3.09
PC1W	199	1	4	26	3	14	0	3	250	0	1	6	43	50	80	12	8
PC1C	212	3	1	11	4	17	0	2	250	0	0	6	44	50	86	4.8	9.2
PC3C	196	3	1	19	4	24	1	2	250	2	1	7	40	50	79.6	8	12.4
PC3S	199	7	5	20	3	13	1	2	250	0	1	8	41	50	82.4	10	7.6
PC4C	185	12	2	27	3	17	1	3	250	1	0	17	32	50	78.8	11.6	9.6
PC4S	189	5	2	31	2	18	2	1	250	0	0	11	39	50	77.6	13.2	9.2
Average	197	5.17	2.5	22	3.17	17.2	0.83	2.2	250	0.5	0.5	9	40	50	80.7	9.9	9.3
Standard deviation	9.40	3.92	1.64	7.15	0.75	3.87	0.75	0.75	0.00	0.84	0.55	4.26	4.26	0.00	3.03	3.09	1.69
V1 F	211	3	3	22	0	11	0	0	250	2	3	33	12	50	85.6	10	4.4
V1 C	201	3	4	23	4	8	2	5	250	0	6	34	10	50	81.6	10.8	7.6
V5 F	214	6	7	19	1	2	0	1	250	0	3	29	18	50	88	10.4	1.6
V5C	201	1	2	31	1	5	3	6	250	1	0	32	17	50	80.8	13.2	6
V9F	216	1	6	14	4	6	1	2	250	5	1	38	6	50	86.8	8	5.2
V9C	215	1	2	18	2	8	1	3	250	7	4	31	8	50	86.4	8	5.6
V13F	198	3	1	30	4	4	4	6	250	5	0	44	1	50	80.4	12.4	7.2
V13C	207	3	2	28	1	4	3	2	250	11	5	30	4	50	84	12	4
Average	208	2.63	3.4	23	2.13	6	1.75	3.1	250	3.9	2.8	34	9.5	50	84.2	10.6	5.2
Standard deviation	7.14	1.69	2.13	6.10	1.64	2.88	1.49	2.30	0.00	3.87	2.25	4.94	6.00	0.00	2.95	1.92	1.91
LB1F	192	3	5	20	5	3	7	15	250	6	2	37	5	50	78	10	12
LB1C	207	4	1	22	4	5	1	6	250	8	4	34	4	50	84.4	9.2	6.4
LB3C	223	8	1	15	0	3	0	0	250	5	3	36	6	50	92.4	6.4	1.2
LB5F	213	4	1	20	2	10	0	0	250	13	1	33	3	50	86.8	8.4	4.8
LB5C	213	9	8	16	2	0	0	2	250	11	2	33	4	50	88.8	9.6	1.6
Average	210	5.6	3.2	19	2.6	4.2	1.6	4.6	250	8.6	2.4	34.6	4.4	50	86.1	8.7	5.2
Standard deviation	11.39	2.70	3.19	2.97	1.95	3.70	3.05	6.31	0.00	3.36	1.14	1.82	1.14	0.00	5.38	1.43	4.38

Qm: monocrystalline quartz; Qp: polycrystalline quartz; Fk: potash feldspar; P: plagioclase; Lv: volcanic lithics (basalt, andesite ?); Ls: sedimentary lithics (sandstone, siltstone, chert,); Lm: metamorphic lithics (schists); Lp: plutonic lithics (granite); Op: opaque minerals (mainly magnetite); Hm: heavy minerals (pyroxenes, hornblende, apatite, ilmenite), Mc: mica (biotite, chlorite); Bg+ C: biogenic debris (mainly shell fragments, foraminifera, calcareous algae) and carbonates (limestone, calcite, dolomite). Qt: total quartz; Ft: total feldspar; Lt: total lithics.

biogenic (broken shells, foraminifera, calcareous algae) plus carbonates (limestone, calcite, dolomite) (Bg + C). In addition, three river samples were also collected near the sites 1, 2 and 9. River sands were collected from the uppermost centimeter in the bed of dry streams at sites close to the main road. The whole bulk sediment was used for point counting of 250 grains. In the case of the dune and river sands, point counts were normalized to 100 % and ternary diagrams for mineralogic (n= 54) and geochemical data (n=24) were plotted for the dune sands data only using confidence regions of the population mean (CRPM) at 95 % confidence level around the mean population of samples. These regions were constructed with the algorithm developed by Weltje (2002) and converted into ellipses by using the Sigma Plot software. The ellipses represent the area in which samples might have variations in relation to the mean. This implies that the CRPM define rigorously if two mean populations are significantly different (Weltje, 2002).

Sand samples (n= 24) were dried at 110º C and treated with lithium metaborate and lithium tetraborate to make pressed powder pellets. They were analysed with a X-ray fluorescence Siemens SRS 3000 equipment for major and trace elements (Table 4). For major and trace elements, precision is valuated in terms of relative standard deviation being <1 % (Sutarno and Steger, 1985). The Chemical Index of Alteration (CIA) values, based on the equation CIA= $100 \cdot [Al_2O_3/(Al_2O_3+CaO^*+Na_2O+K_2O)]$ (Nesbitt and Young, 1982), were obtained using the CaO^* values present only in the silicate fraction (Honda, electronic communication). No geochemical data were available for

Table 3. Point counts and percentages of the major constituents of some river samples.

	ET river 114º02'W 28º30'N	SP river 113º25'W 27º44'N	PO river 113º15'W 27º25'N	Average	Standard deviation
Qm	71	190	90	117	63.93
Qp	25	6	2	11	12.29
Fk	7	15	3	8.33	6.11
P	29	12	28	23	9.54
Lv	33	13	90	45.3	39.95
Ls	29	12	31	24	10.44
Lm	21	0	0	7	12.12
Lp	35	2	6	14.3	18.01
Total	250	250	250	250	0
Op	1	25	2	9.3	13.58
Hm	0	5	1	2	2.65
Mc	9	19	1	9.7	4.62
Bg+C	10	1	0	3.7	9.5
Total	20	50	4	24.6	23.35
Qt	38.4	78.4	36.8	51.2	23.57
Ft	14.4	10.8	12.4	12.5	1.8
Lt	47.2	10.8	50.8	36.3	22.13
Total	100	100	100	100	0
Lv	28	48.1	70.9	49	21.46
Ls	24.6	44.4	24.4	31.1	11.52
Lm	17.8	0	0	5.9	10.27
Lp	29.7	7.4	4.7	13.9	13.69
Total	100	100	100	100	0

See Table 2 for abbreviations. Point counts of Op, Hm, Mc and Bg+C in the ET and PO rivers could not achieve 50 grains. ET: El Tomatal, SP: San Pablo, PO: El Porvenir.

surrounding/parental rocks. Correlations were established between textural, mineralogic and geochemical parameters. However, we should mention that discordancy tests for the correlations were not carried out, which implies that rejection or identification of outliers of special interest could not be established (Barnet and Lewis, 1994, Verma, 1997; Verma and Quiroz-Ruiz, 2006).

RESULTS

El Vizcaíno dune sands characteristics

According to the field observations and satellite images, coastal and desert dunes were separated on the basis of the physiography of the area. Coastal dunes are located mainly near beaches of the Vizcaíno Bay (sites 1-7). They are of transverse (sites 1, 2, 4, 6) and barchan types (sites 3, 4, 5, 7) Inland desert dunes are vegetated sand sheets with little morphological definition but probably parallel to the dominant wind direction (sites 8-9) (Figure 1B). Mobile dunes are located in sites 3, 5 and 7 whilst the rest of the dune sites are semi-mobile vegetated systems. The average heights for the coastal and desert dunes are 7.7 m and 14.0 m above sea level respectively.

Grain size distributions

Average grain size parameters for each sampling site are presented in Table 1. The average grain size for the coastal desert sands is 2.434 ϕ, sorting is 0.466 ϕ, skewness is -0.040, and kurtosis is 1.025. The average grain size for the inland dune sands is 2.520 ϕ, sorting is 0.476 ϕ, skewness is 0.028, and kurtosis is 1.015 (Table 1). The grain size correlations among textural parameters for the El Vizcaíno Desert dune sands show that there are only two significant correlations between grain size, sorting and grain size and skewness (Khalaf, 1989; Kasper-Zubillaga and Carranza-Edwards, 2005) (Figure 2).

Mineralogy

The compositional framework of the sands consisted of monocrystalline (Qm) and polycrystalline quartz (Qp), potassium feldspar (Fk), plagioclase (P), volanic (basalt, andesite) (Lv), sedimentary (sandstone, siltsone, chert) (Ls), metamorphic (schist) (Lm) and plutonic lithics (granite) (Lp). The El Vizcaíno Desert coastal dune sands are quartzolithic sands (Qt_{82} Ft_{14} Lt_4) (Figure 3). Average lithic percentages are 67 %, 18 % and 15 % for Ls, Lv and Lm+Lp respectively. Mica and biogenic detritus plus carbonates are abundant with 47 % and 42 % content in relation to opaque and heavy minerals (2 % to 9 %, respectively) (Table 2).

The El Vizcaíno inland dune sands are quartzolithic

Table 4. Average and standard deviation values of major element (in wt. %) and trace elements analyses (in ppm).

	Average coastal dunes	Standard deviation	Average desert dunes	Standard deviation
SiO_2	70.39	2.964	71.38	1.152
TiO_2	0.34	0.228	0.35	0.072
Al_2O_3	13.25	1.039	14.24	0.699
Fe_2O_3	2.09	1.358	1.92	0.372
MnO	0.03	0.032	0.01	0.013
MgO	1.09	0.546	0.94	0.258
CaO	5.68	2.022	4.74	0.632
Na_2O	3.33	0.326	3.52	0.17
K_2O	1.31	0.218	1.44	0.222
P_2O_5	0.31	0.176	0.5	0.434
Rb	62.5	11.888	45.6	9.453
Sr	532.83	154.54	480.6	45.654
Ba	507.89	56.26	581.4	83.502
Y	51.833	18.398	29.6	3.933
Zr	146	50.1	171	27.792
Nb	25.33	9.133	12.8	2.608
V	53.7	45.6	43	11.1
Cr	26.44	18.89	26.8	8.892
Co	144.7	48.75	56	11.583
Ni	34.6	8.211	19.6	3.266
Cu	22.7	5.41	11.4	3.327
Zn	44	23	28.8	5.762
Pb	7.5	1.1	8.8	1.941

sands ($Qt_{85}\ Ft_{10}\ Lt_5$)(Figure 3). Average lithic percentages are 43 %, 20 % and 37 % for Ls, Lv and Lm+Lp respectively. Point counts of accessory minerals show an increase in the mica content compared to the rest of the trace components (Table 2). Mica and biogenic detritus plus carbonates content is 68 % and 15 % content, respectively, whereas opaque and heavy minerals are 11 % and 15 %, respectively.

The Q-F-L diagram (Dickinson *et al.*, 1983) shows that the coastal and inland dune sands plot in the craton interior and recycled orogen fields (Figure 4).

Geochemistry

Similar major elements values are presented for coastal and inland dunes sands (Tables 5, 6). However there are higher values of trace elements like Rb, Sr, Y, Co, Ni, Cu and Zn for coastal dune sands compared to the inland dune sands (Table 6).

The A-B-C ternary diagram with CRPM, where A is SiO_2, B is K_2O+Na_2O+Al_2O_3, and C is Fe_2O_3+TiO_2+MgO, shows a dispersal towards the A-B poles for the coastal dune sands (Figure 5a). Average content of SiO_2 is 76 %. In the CaO-Na_2O-K_2O ternary diagram, the content of CaO, Na_2O and K_2O is 53% and 34 % and 13 %, respectively. The slight dispersal of the CRPM is towards the K_2O pole (Figure 5b).

The A-B-C ternary diagram with CRPM shows a dispersal towards the A-B poles with similar percentages in A-B-C for the inland dune sands compared to the coastal dune sands. (Figure 5a). The CaO-Na_2O-K_2O ternary diagram shows a slight increase in K_2O and abrupt dispersal of the CRPM towards the K_2O pole compared to the coastal dune sands (Figure 5b).

The CIA-A-CN-K triangle (Nesbitt and Young, 1996) shows that most of the coastal and inland dune sand samples tend towards the A pole, representing the Al_2O_3 concentration, with relatively low CIA values (Figure 6)

The K_2O/Na_2O *vs.* SiO_2/Al_2O_3 diagram (Roser and Korsch, 1986) indicates that some coastal and inland dune sand samples plot in the evolved arc setting felsic-plutonic detritus field and in the active continental margin arc, and passive margin fields (Figure 7).

The Ni *vs.* Ti plot (Floyd *et al.*, 1989; Nagarajan *et al.*, 2007) shows that the overall of the coastal and inland dune sand samples are placed in the mature sediments fields with only three samples in the acidic source field (Figure 8)

DISCUSSION

Grain size distribution

The coastal and inland dune sands are fine, well sorted, near symmetrical sands with mesokurtic distributions. Similar patterns in coastal and desert dune sands have been reported in dune systems from five continents where dune sands are well sorted fine sands with symmetrical distributions and mesokurtic curves (Ahlbrandt, 1979).

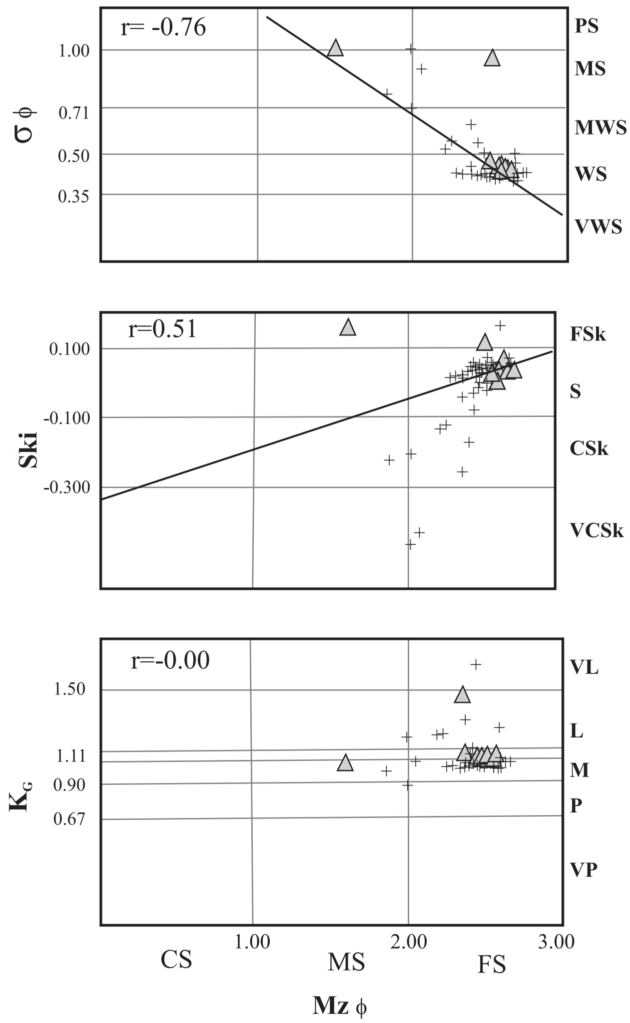

Figure 2. Binary diagrams of grain size (Mz) vs. sorting (σ), skewness (Ski) and kurtosis (K_G). Values (r) are the Pearson correlation coefficients that assess the degree to which two variables are related. Crosses represent coastal dunes; shaded triangles represent desert dunes. PS: poorly sorted; MS: moderately sorted; MWS: moderately well sorted; WS: well sorted; VWS: very well sorted. FSk: fine skewed; S: Skewed; CSk: coarse skewed; VCSk: very coarse skewed. VL: very leptokurtic; L: leptokurtic; M: mesokurtic; P: platikurtic; VP: very platikurtic. CS: coarse sand; MS: medium sand; FS: fine sand.

The El Vizcaíno coastal and inland dune sands suggest that the sands have experienced an aeolian process due to westerly and northerly onshore winds, which might have caused that the dune sands have retained some of the beach sands textural characteristics as it is observed by the fine-grained and well-sorted values (average= 2.6 ϕ; sorting= 0.42 ϕ) (Carranza-Edwards *et al.*, 1998). The onshore wind patterns with velocities of 2 to 6 $m \cdot s^{-1}$ and 40 % of frequency might control the fine-sized and well-sorted distributions of the dune sands. This can be supported by the fact that threshold velocities in fine to medium sands

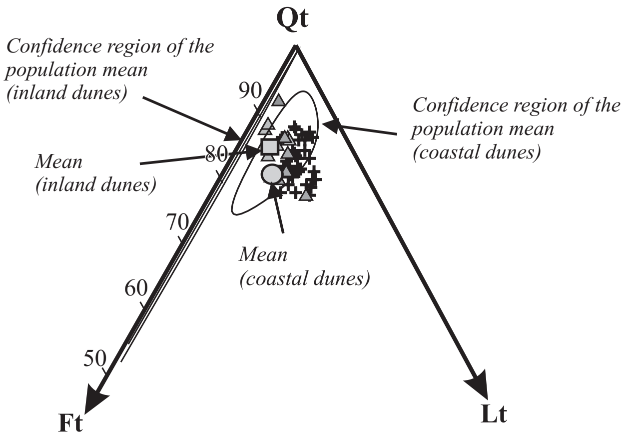

Figure 3. Qt-Ft-Lt ternary diagram with samples from the El Vizcaíno Desert coastal and desert dune sands. Qt: total quartz; Ft: total feldspar; Lt: total lithics. Confidence regions of the population mean are at 95 % confidence level. Crosses: coastal dunes; shaded triangles: desert dunes.

are above 4 $m \cdot s^{-1}$. This suggests that the fine-sized beach sand grains might have experienced a short transport after their removal from the beach into the dune systems, leaving their textural characteristics similar to those observed for the beach sands. The grain size distributions of coastal and inland dunes indicate that the dune sands are not grain size selective when the beach sediments are fine grained and well sorted (Pye 1991).

Mineralogy

The CRPM shape of coastal dune sands, compared to the inland sands, suggests more concentration of coastal sand samples near the mean population compared to the inland dune sands, but this is also due to the higher number of samples for the costal dune sands (Figure 3). These shapes are associated with the amount of dispersal of data plotted in the ternary diagram (Weltje , 2002). The CRPM quantitative approach reveals that coastal and inland dune fields are not significantly different. The enrichment of quartz in both dune systems within the El Vizcaíno desert basin probably resulted from the maturity process, where the source rock might provide quartz-rich sediments. This interpretation is supported by 1) the presence of the alluvial deposits in the El Vizcaíno basin underlying the dune fields; 2) the composition of some of the rivers draining throughout the basin with moderately high quartz content; 3) the high content of sedimentary lithics probably derived from sedimentary outcrops in the area, but also from the alluvial deposits that provides quartz detritus to the coastal and desert dune sands; and 4) the presence of quartz-rich beach sands (Qt_{90} Ft_9 Lt_1) near sites 1 to 7 that might contribute to the landward transport of beach sands by the wind (Carranza-Edwards *et al.*, 1998). Moreover, the Q-F-L plot (Dickinson *et al.*, 1983) indicates a craton interior and recycled orogen with tectonic fields suggesting intrusive, sedimentary and partly metamorphosed sources (Dickinson *et al.*, 1983; Amstrong-Altrin *et al.*, 2004) (Figure 4). Maturation of the sands may be related to secondary processes as wind action leads to quartz-rich dune sands (Muhs, 2004; Kasper-Zubillaga *et al.,* 1999). Furthermore, some samples from the inland dune sands (V9C, V13C, LB5F) have been probably influenced by some eroded acid, volcanic, and metamorphic (schist) rocks, as well as by acid-intermediate plutonic rocks like the granitic and granodiorite outcrops in the north of the El Vizcaíno Desert basins. The alluvial deposits in the El Vizcaíno Desert were mainly derived from the above mentioned rock types. This is especially observed for the volcanic lithic fractions. From the alluvial deposits, the wind transports sediment towards the inland dune sands. Also, the release of mica and hornblende in the inland dune sands might support the influence of granitic, granodiorite and schist sources to the alluvial deposits, and consequently to the dune sands during short aeolian transport. This is especially observed in the San Pablo (SP) river, where mica is a relatively important constituent of fluvial sands and where plutonic and metamorphic fractions are depleted (Table 3).

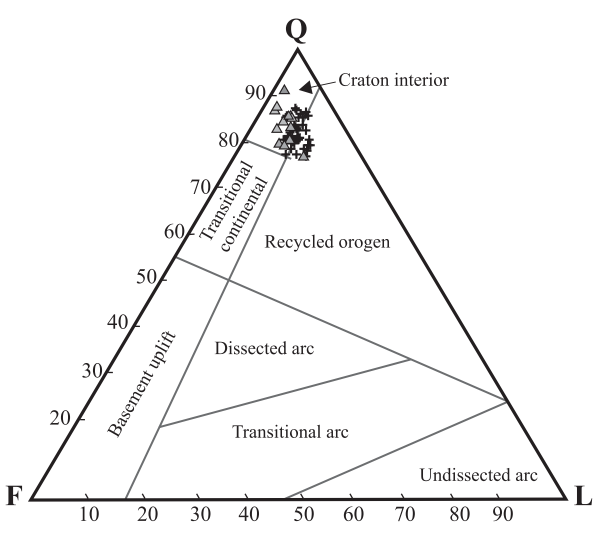

Figure 4. Q-F-L diagram (Dickinson *et al.*, 1983) for tectonic setting signals. Q: quartz, F: feldspar, and L: lithics. Crosses: coastal dunes; shaded triangles: desert dunes.

The presence of carbonate shells in the coastal dune sands indicates the beach sand influence in the composition of these sands. It is likely that the northwesterly and northerly winds are capable of transporting shell fragments onto the dune fields of the coast. The amounts of broken shells and carbonate minerals like calcite are depleted landward as result of their softness and long transport by the wind.

Geochemistry

In the A-B-C ternary diagram (Figure 5a), it is observed that the compositions of the coastal and desert

Table. 5. Major element analyses and CIA values for the El Vizcaíno coastal and inland desert dune sands (values in wt. %) (*n*= 24).

Sample	SiO_2	TiO_2	Al_2O_3	Fe_2O_3	MnO	MgO	CaO	Na_2O	K_2O	P_2O_5	LOI	CIA
PPN1F	67.18	0.91	13.00	5.91	0.08	1.95	4.28	2.47	1.99	0.13	1.43	62.71
PPN3C	68.44	0.54	13.40	4.26	0.08	2.41	5.58	3.03	0.92	0.15	0.66	58.56
PPS7F	74.73	0.24	12.99	1.65	0.00	0.77	3.77	3.27	1.27	0.14	0.87	55.94
LM1W	70.52	0.38	12.99	2.44	0.02	1.24	5.42	3.28	1.23	0.65	1.02	55.86
LM5C	71.27	0.52	13.27	2.81	0.03	1.47	4.82	3.37	1.22	0.25	0.69	55.72
LM7S	73.57	0.30	13.30	2.14	0.01	1.14	4.32	3.30	1.19	0.16	0.74	56.29
LG1W	72.12	0.25	13.70	1.57	nd	0.89	4.01	3.45	1.35	0.17	2.96	55.93
LG3C	71.69	0.40	13.69	2.05	0.00	1.09	4.94	3.44	1.37	0.52	0.68	55.98
LG7F	70.62	0.45	14.52	2.35	0.02	1.26	4.73	3.56	1.33	0.18	0.60	56.59
IA1W	67.42	0.17	12.79	1.01	nd	0.54	8.37	3.49	1.41	0.65	3.96	53.94
IA3C	69.51	0.17	14.21	1.03	nd	0.64	6.49	3.70	1.55	0.30	2.61	55.10
IA5S	72.48	0.17	14.14	1.09	nd	0.61	4.79	3.78	1.46	0.19	1.43	54.45
ES1C	71.32	0.37	13.60	2.23	0.02	1.36	4.92	3.36	1.15	0.24	0.83	56.40
ES5F	73.96	0.19	13.57	1.41	nd	0.87	4.55	3.42	1.24	0.27	0.89	55.91
ES6C	68.08	0.78	13.76	3.36	0.07	1.76	5.78	3.34	1.15	0.30	1.37	56.83
PC1W	62.56	0.09	9.89	0.55	nd	0.36	11.95	2.75	1.20	0.56	6.66	53.47
PC3C	68.97	0.15	11.83	0.79	nd	0.56	8.30	3.24	1.31	0.45	4.20	53.85
PC4S	72.51	0.12	13.88	0.89	nd	0.74	5.14	3.74	1.28	0.32	1.72	54.26
V1F	71.66	0.28	14.56	1.64	nd	0.89	4.66	3.63	1.31	0.25	0.82	56.18
V5C	72.04	0.36	14.59	1.91	0.01	1.00	4.81	3.56	1.33	0.30	0.85	56.71
V13C	69.48	0.47	15.02	2.66	0.03	1.43	5.03	3.63	1.29	0.29	0.64	56.94
LB1F	71.95	0.28	14.41	1.73	nd	0.71	3.85	3.67	1.87	0.31	0.87	55.65
LB3C	72.59	0.32	13.83	1.79	0.00	0.80	4.35	3.35	1.47	0.45	0.87	56.88
LB5F	70.53	0.38	13.05	1.81	0.01	0.82	5.72	3.26	1.35	1.37	1.24	56.13
Detection limits	0.050	0.004	0.018	0.006	0.004	0.015	0.040	0.030	0.050	0.004		

LOI: loss on ignition; CIA: chemical index of alteration (Nesbitt and Young, 1982; see text). nd: undetermined or values below the lower limit of detection.

Table 6. Trace elements analyses of the El Vizcaíno coastal and inland desert dune sands (values in ppm) (*n*= 24).

Sample	Rb	Sr	Ba	Y	Zr	Nb	V	Cr	Co	Ni	Cu	Zn	Pb
PPN1F	59	267	593	29	137	11	204	85	49	33	30	58	6
PPN3C	35	386	378	55	115	19	116	48	93	33	12	83	9
PPS7F	58	425	500	41	119	26	48	18	122	31	18	38	8
LM1W	60	493	505	67	135	27	57	35	144	37	22	59	7
LM5C	74	488	472	90	174	39	62	34	212	48	27	75	6
LM7S	87	511	496	92	110	51	58	26	275	60	34	63	6
LG1W	66	457	557	45	122	23	35	18	129	32	21	36	9
LG3C	71	530	548	69	184	34	49	26	168	37	23	46	7
LG7F	60	471	547	54	194	25	66	27	126	35	19	54	8
IA1W	66	667	520	43	127	22	17	16	146	28	25	23	7
IA3C	81	621	587	46	119	22	32	13	161	35	26	31	8
IA5S	65	517	571	36	107	14	27	19	116	26	19	27	10
ES1C	54	494	485	56	155	25	53	31	142	36	21	55	7
ES5F	53	478	520	37	111	17	29	18	108	27	17	29	7
ES6C	50	475	428	63	316	27	71	42	121	36	17	77	8
PC1W	60	992	437	33	150	28	13	1	186	32	27	<1.5	7
PC3C	56	736	496	35	144	22	13	10	137	25	22	12	7
PC4S	70	583	502	42	106	24	16	9	170	32	28	25	8
LB1F	63	562	745	32	150	13	50	29	74	24	18	31	11
LB3C	42	425	558	27	152	9	36	31	41	16	10	30	11
LB5F	39	489	532	36	208	11	41	32	48	18	10	29	8
VIF	42	464	535	25	148	15	40	17	55	19	10	25	8
V5C	42	463	537	28	198	16	48	25	62	21	9	29	6
V13C	37	473	547	30	194	14	67	44	51	24	11	42	9
Detection limits	2	1	11	0.5	0.5	0.7	5	2	3	0.5	0.7	1.5	5

sands overlap, which can be attributed to the maturity of the dune sands near and away from the coast. This can be visualized by the high SiO_2 contents and relatively similar mineralogical composition of feldspar and lithic fractions for both dune types. The CaO-Na_2O-K_2O diagramm shows no significant differences between the coastal and desert dune sands (Figure 5b). The K_2O content in the desert dune sands might be associated with the presence of mica, and dispersal of the CRPM towards the K_2O pole may be due to the different amount of mica in the samples. Furthermore, low concentration of potassium feldspar in the El Vizcaíno dune sands (Table 2) might be associated with the composition of the beach and alluvial deposits that provide little K-feldspar. This is also related to the chemical composition of the northern beach sands that in the overall have more than 60% of CaO, derived from plagioclase, and less than 30 % of K_2O, associated with potassium feldspar (Carranza-Edwards *et al.*, 1998).

In addition, the Chemical Index of Alteration (CIA) values obtained for the sand samples indicate low chemical

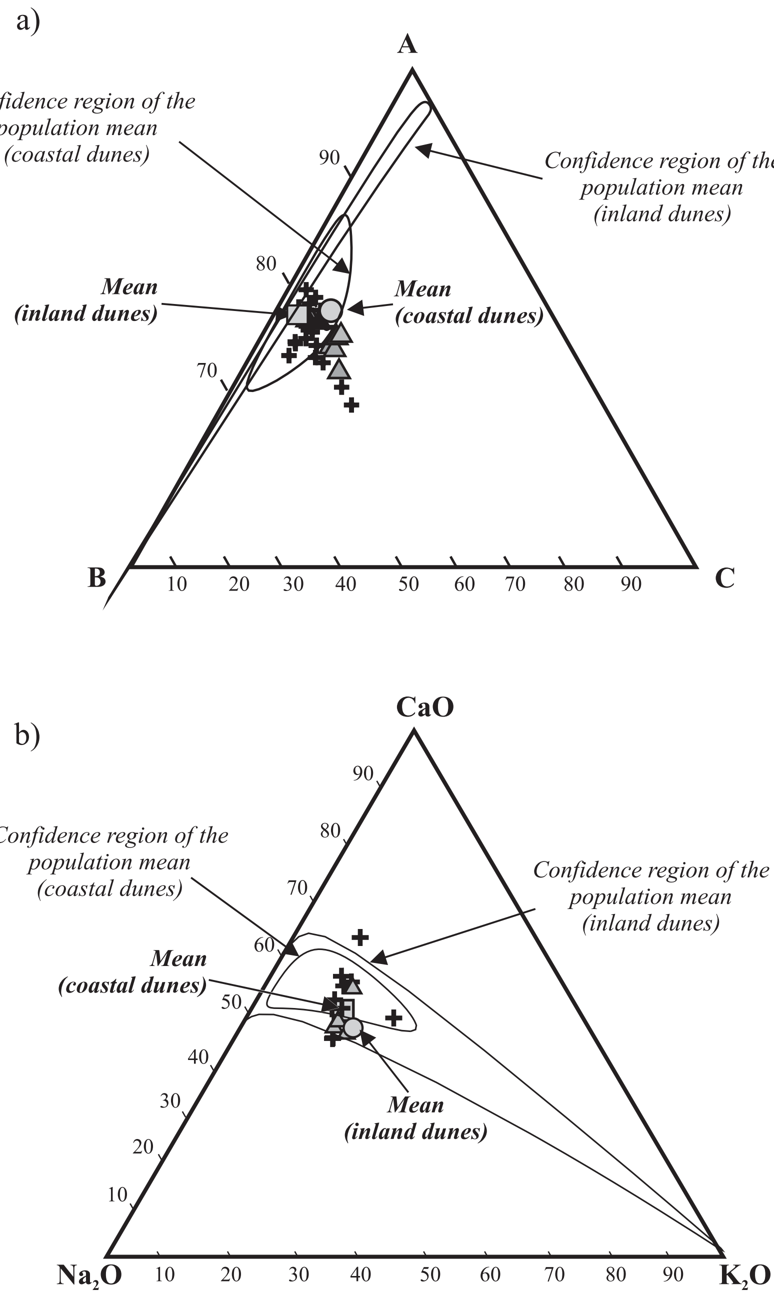

Figure 5. a) A-B-C ternary diagram for the El Vizcaíno Desert coastal and inland sands where A= SiO_2 , B= $K_2O + Na_2O + Al_2O_3$ and C= $Fe_2O_3+TiO_2+MgO$. b) CaO-Na_2O-K_2O ternary diagram for the El Vizcaíno Desert coastal and inland sands. Confidence regions of the population mean are at 95 % confidence level. Crosses: coastal dunes; shaded triangles: desert dunes.

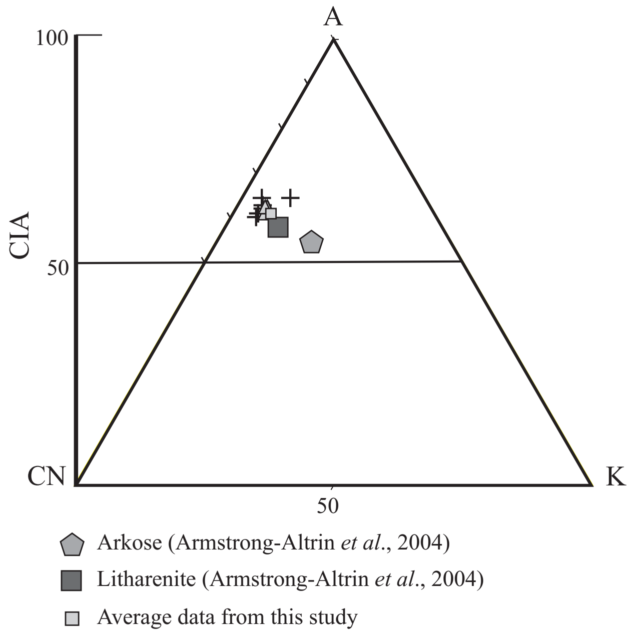

Figure 6. CIA-A-CN-K triangle (Nesbitt and Young 1982). See text for explanation. Crosses: coastal dunes; shaded triangles: desert dunes. Average data for sandstones of the Kudanculam Fm., India, reported by Armstrong-Altrin *et al.* (2004) are showed for comparison.

weathering for the coastal and inland dune sands (Figure 6). The ACNK diagram indicates that, in the overall, El Vizcaíno sand samples have experienced low chemical weathering probably because of the dryness of the area. El Vizcaíno dune sands have similar CIA values to those observed in arkose and litharenites from ancient sandstones in India (Armstrong-Altrin *et al.*, 2004).

The presence of Rb, Sr and Ba in both dune systems is probably associated with the presence of mica and, in lesser extent, of potash feldspars. This is because Rb, Sr and Ba are trace elements that may substitute for K in the lattice of mica and potash feldspar (Sawyer, 1986; Gallet *et al.*, 1996; Canfield, 1997; Muhs *et al.,* 2003). Yttrium may be associated with the presence of basaltic and metamorphic sources in the coastal dune sands (Hawkesworth and Morrison, 1978; Hill *et al.*, 2000).

The enrichment in Co in the coastal dunes may be related to the recycling of sedimentary lithics within sand samples near marine environments, where correlation between Co and Ls is relatively significant (r= 0.72). This is because some sedimentary lithics can be potential carriers of some accessory minerals like opaques and heavy minerals that may concentrate Co under marine weathering conditions because of the immobility of Co in aqueous conditions (Zolezzi-Ruiz, 2007). Furthermore, Co may be associated with the presence of titanium and iron oxides (Krupka and Serne, 2002) in the sedimentary lithics composed of accessory minerals like rutile, sphene, Ilmenite and magnetite. This is evidenced by 1) the high concentrations of Co in sand samples coming from the sites 2, 3, 4, 5, 6, and 7, near the coastal areas with marine influence; and 2) the presence of titanium and iron minerals in the El Vizcaíno dune sands. Ni, Cu and Zn may be associated with the presence of sedimentary lithics in the coastal dune sands, which may contain some opaque and heavy minerals probably associated to ultramafic rocks (Lee, 2002; Zolezzi-Ruiz, 2007).

Correlations between Fe_2O_3, TiO_2, MgO and V (Figure 9) indicate the following: 1) The positive correlation between Fe_2O_3, TiO_2, and MgO suggests the presence of heavy minerals associated with sedimentary sources mainly ilmenite and magnetite (Basu and Molinaroli, 1989; Carranza-Edwards *et al.*, 2001); 2) the positive correlations between TiO_2, Zr and V suggests that the sands are influenced by magnetite, ilmenite and zircon minerals associated with some other heavy minerals probably derived from sedimentary-volcanic sources. In both cases, similar correlations have been observed in dune and beach sands in the Gulf of Mexico coast, the Mexican western coast and northwestern Mexico (Kasper-Zubillaga *et al.*, 1999; Carranza-Edwards *et al.*, 2001; Kasper-Zubillaga *et al.*, 2006b). In the El Vizcaíno dune sands, velocity and frequency of the winds might transport magnetite and some other heavy minerals landward. This process has been also observed for the Altar Desert dune sands close to the Colorado Delta River in northwestern Mexico, where short aeolian transport enables the transport of heavy minerals from the source sediment to the dune system (Kasper-Zubillaga *et al.*, in press).

Comparisons of dune fields from El Vizcaíno Desert with other North American Deserts

Quartz percentages in the El Vizcaíno dune sands are similar to those found in the Altar Desert dune sands in northwestern Mexico (Kasper-Zubillaga *et al.,* 2006b) with a slight enrichment in plagioclase minerals (Figures 10a, b). The data plotted in a Qt-Ft-Lt ternary diagram with

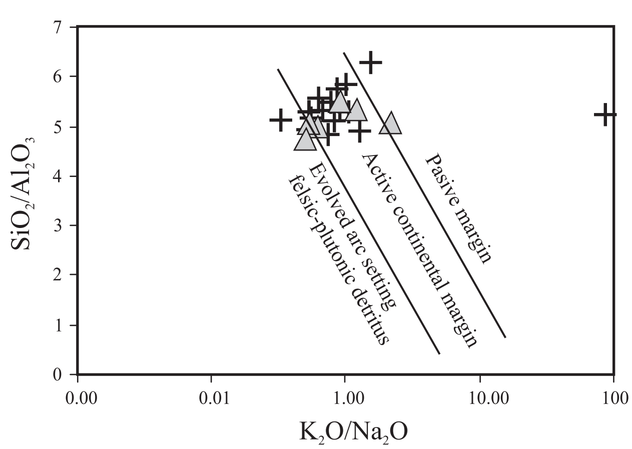

Figure 7. K_2O/ Na_2O *vs.* SiO_2 /Al_2O_3 diagram for provenance and tectonic setting (Roser and Korsch, 1986). Crosses: coastal dunes; shaded triangles: desert dunes.

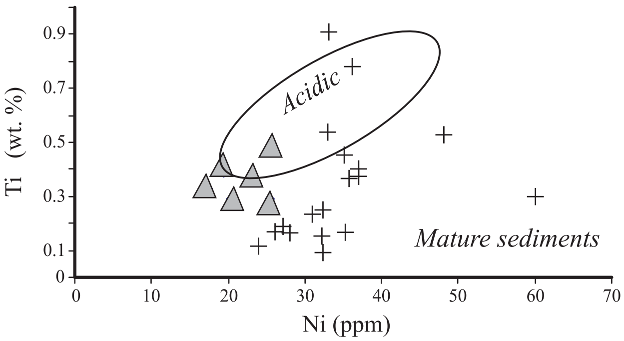

Figure 8. Ni (ppm) *vs.* Ti (%) plot (Floyd *et al.*, 1989) for provenance signals. Crosses: coastal dunes; shaded triangles: desert dunes.

the CRPM show that the El Vizcaíno sands tend slightly towards the total feldspar pole. The CRPM for both sites do not overlap, which suggests that dune sands from both areas are significantly different (Figure 10b).

One source of the El Vizcaíno dune sands are probably beach sands in turn derived mainly from sedimentary (alluvial) and, in lesser extent, by metamorphic and plutonic sources exposed near the El Vizcaíno Desert. Some volcanic lithics also contribute to the dune composition but the release of monomineralic crystals of plagioclase, some pyroxenes, hornblende and opaque minerals are important constituents of the dune sands despite the short aeolian transport, especially in the coastal dunes (Akulov and Agafonov, 2007). The slight enrichment in plagioclase and lithics in the El Vizcaíno dune sands might derive from the alluvial deposits. This is evidenced by the large content of sedimentary lithics in the El Vizcaíno dune sands and also by the extensive area in which the alluvial deposits outcrop north of the El Vizcaíno. When comparing the Vizcaíno dune sands with the Altar Desert dune sands in Sonora, the CaO-Na_2O-K_2O diagram (Figure 11) shows that El Vizcaíno dune sands follow the CaO-Na_2O line, whereas the Altar Desert dune sands follow slightly the CaO-K_2O trend and approaches towards the K_2O peak. High content of CaO-Na_2O in the El Vizcaíno Desert dune sands is again probably due to the slight enrichment of plagioclase feldspar.

An A-B diagram was plotted for different dune systems of North America where A= SiO_2 and B= K_2O+ Na_2O+Al_2O_3. The El Vizcaíno Desert dune sands are higher in B content compared to the Altar Desert dune sands, the Algodones and Parker dunes and the Colorado River sediments (Muhs, 2004; Kasper-Zubillaga *et al.*, 2006) (Figure 12). Likewise, the El Vizcaíno dune sands lay within the range of A and B content (with the exception of sample ES5F) of the Rice Valley dunes in California (Muhs, 2004). In the case of the El Vizcaíno dune sands, high B content is probably associated with the presence of mica in the sands High mica content in the El Vizcaíno dune sands indicates that wind velocity

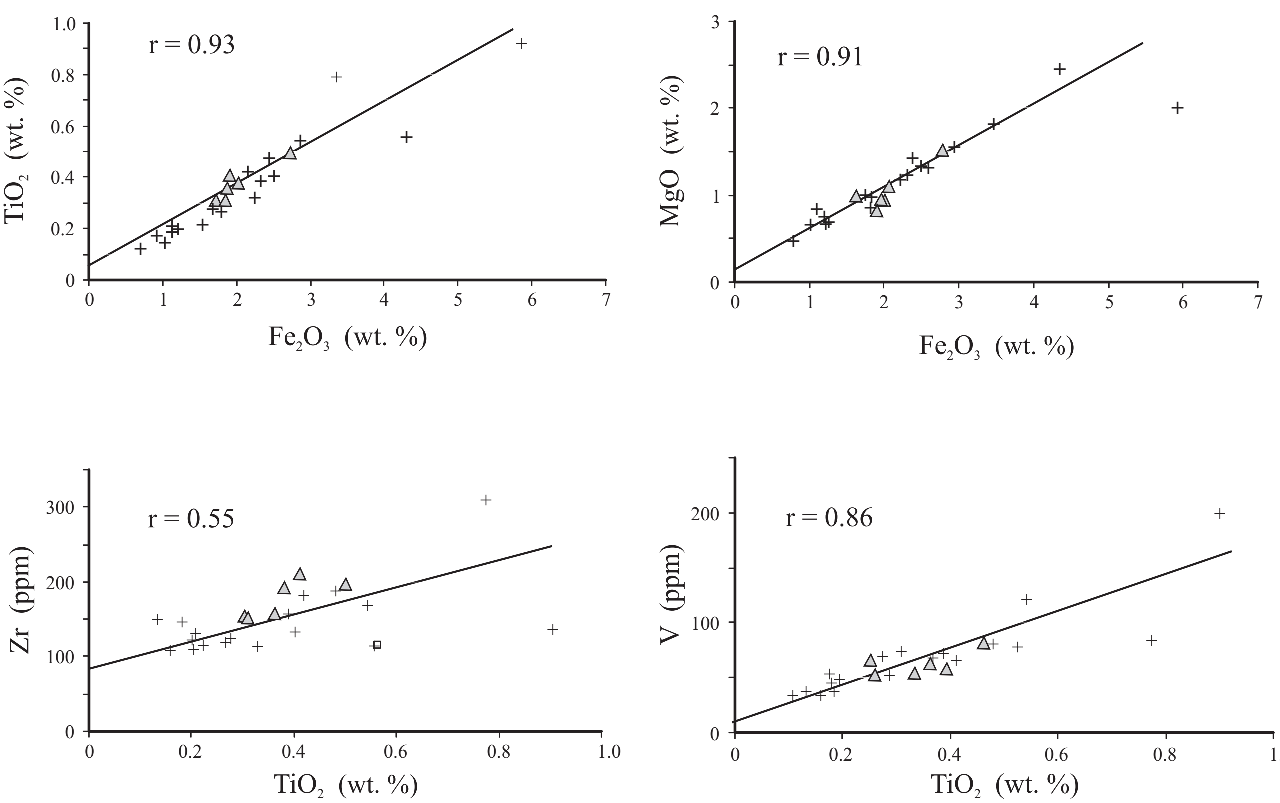

Figure 9. Pearson correlations between Fe_2O_3, TiO_2, MgO, Zr, V, Rb and Ba for the El Vizcaíno Desert dune sands. Crosses: coastal dunes; shaded triangles: desert dunes.

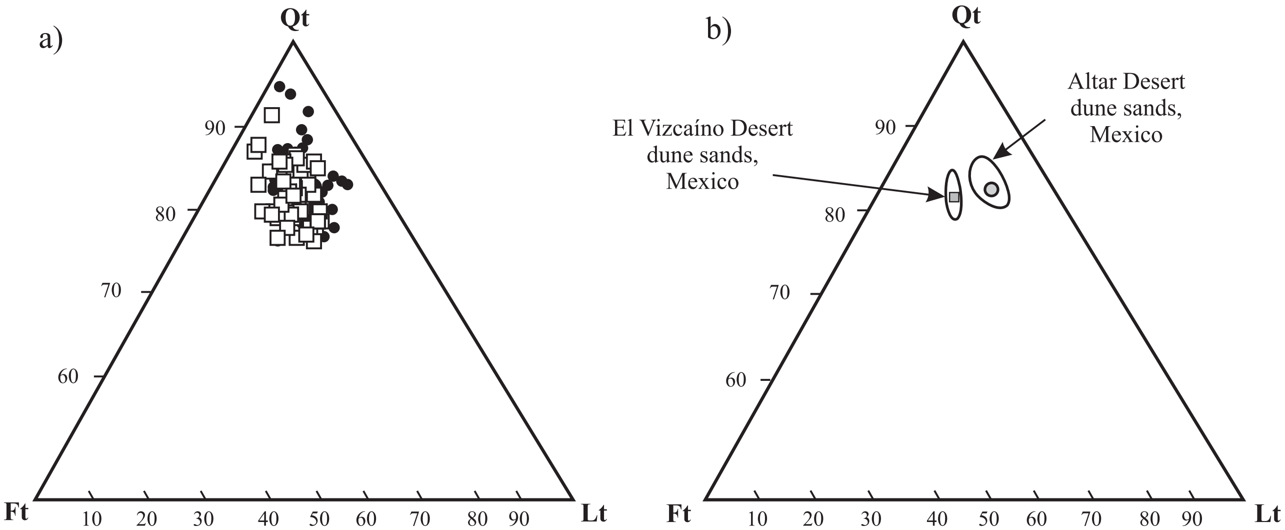

Figure 10. a) Qt-Ft-Lt ternary diagram with samples from the El Vizcaíno Desert dune sands (open squares) and the Altar Desert dune sands (filled circles), b) Average for the El Vizcaíno and the Altar Desert dune sand samples are represented by a shaded square and by a shaded circle, respectively. The elipses represent the confidence regions of the population mean are at 95 % confidence level.

exerts a control in the composition of the sands carrying beach and alluvial sands into the dune systems. perhaps enhanced by the platy morphology of the micas.

In addition, the low chemical index of alteration values in the El Vizcaíno Desert, similar to those in the Rice Valley dunes (Muhs 2004), indicate that the plagioclase content might be preserved in the sands. This is evidenced by the content of Na_2O. In contrast, dune sands from the Altar Desert and Algodones have inherited their maturity from the silica-rich Colorado River Delta sediments (Muhs 2004; Kasper-Zubillaga *et al.*, 2006, in press).

CONCLUSIONS

1. The El Vizcaíno dune sands are fine, well sorted, near symmetrical sands with mesokurtic distributions. This reflects that onshore wind frequencies and velocities produce fine-sized and well-sorted dune sands inherited from beach sands during short aeolian transport into the coastal and inland dunes.

2. The El Vizcaíno coastal and desert dune sands are placed in the craton interior and recycled orogen fields in the Q-F-L- triangle, which suggest intrusive, sedimentary and partly metamorphosed sources have contributed to the composition of the sands. The presence of minerals like mica and hornblende in the bulk composition of the dune sands supports the influence of granitic, granodioritic and schistose sources. The presence of biogenic detritus and carbonates in the coastal dune sands suggests that they are derived from beach sand sources mixed with alluvial deposits, whereas the inland desert dune sands are derived from alluvial deposits derived from sedimentary, volcanic, schists and granitic and granodiorites.

3. Maturity of the El Vizcaíno dune sands is inherited from the alluvial and beach sands of the Vizcaíno Bay and the desert basin, despite the complex lithology surrounding the dune fields. Maturity of the dune sands is related to aeolian/marine processes.

4. The geochemistry of the El Vizcaíno dune sands show that the dune sands are associated with acid, felsic-plutonic detritus linked to an active continental margin. Low CIA values are related to the dry climate of the area. The high concentrations of Rb, Sr, Ba, Y, Co Ni, Cu and Zn in the coastal dune sands are probably associated with the presence of mica, basaltic and metamorphic sources,

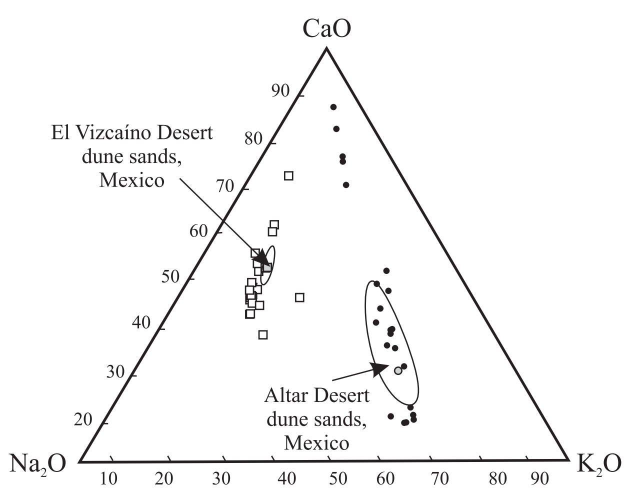

Figure 11. CaO-Na_2O-K_2O ternary diagram for El Vizcaíno (open squares) and the Altar Desert dune sands (filled circles). Average for the El Vizcaíno and the Altar Desert dune sand samples are represented by a shaded square and by a shaded circle, respectively. The elipses represent the confidence regions of the population mean are at 95 % confidence level.

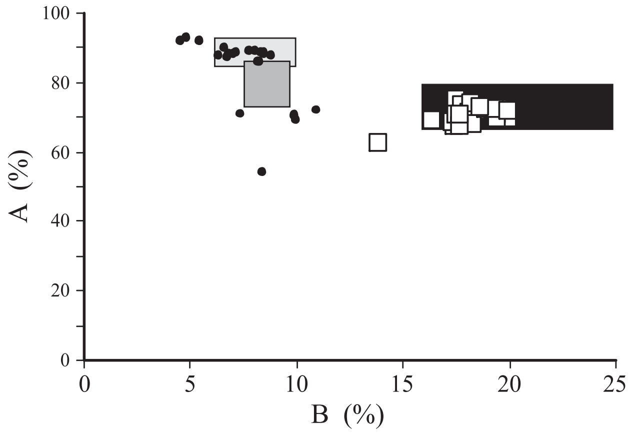

Figure 12. A *vs*. B diagram showing the trends of the Vizcaíno (open squares) and the Altar Desert dune sands (filled circles). A= SiO_2; B= $K_2O+Na_2O+Al_2O_3$. The diagram also shows the range of samples from Rice Valley dunes (black shaded rectangle) and the Algodones and Colorado River sediments (gray shaded square) and Parker dunes (light shaded rectangle) (Muhs, 2004).

sedimentary lithics containing titanium and iron minerals, opaques and heavy minerals. Correlations between Fe_2O_3, TiO_2, MgO, Zr and V in the dune sands indicate the presence of ilmenite, magnetite and zircon in the sands.

ACKNOWLEDGEMENTS

We are indebted to the Instituto de Ciencias del Mar y Limnología, UNAM, for the financial support (internal project 109, Marine processes in coastal sedimentary environments). We are also grateful to Eduardo Morales de la Garza for his invaluable assistance during the particle size analysis. We are indebted to Dr. Thomas E. Gill and Dr. J. Madhavaraju for their invaluable review of this paper.

REFERENCES

Ahlbrandt, T.S., 1979, Textural parameters of eolian deposits, *in* McKee, E.D. (ed.), A Study of Global Sand Seas: Washington, United States Geological Survey, Professional Paper, 1052, 21-58.

Akulov N.I., Agafonov, B.F., 2007, The behavior of heavy minerals in lithostream: Russian Geology and Geophysics, 48, 267-271.

Armstrong-Altrin, J.S., Lee, I.Y., Verma, S.P., Ramasamy, S., 2004, Geochemistry of sandstones from the Upper Miocene Kudankulam Formation, Southern India: implications for provenence, weathering and tectonic setting: Journal of Sedimentary Research, 74, 285-297.

Bagnold R.A., 1941, The Physics of Blown Sand and Desert Dunes: London, Methuen, 265 p.

Basu, A., Molinaroli, E., 1989, Provenance characteristics of detrital opaque Fe-Ti oxide minerals: Journal of Sedimentary Research, 59, 922-934.

Blount G., Lancaster N., 1990, Development of the Gran Desierto sand sea: Geology, 18, 724-728.

Barnett, V., Lewis, T., 1994, Outliers in statistical data: Chichester, John Wiley & Sons, 584 p.

Buoy Weather, 2005, A Global Weather Service (en línea): http://buoyweather.com, accessed on July 4, 2005, 13.00 hrs.

Canfield, D.E., 1997, The geochemistry of river particulate from USA: major elements: Geochimica et Cosmochimica Acta, 61, 3349-3365.

Carranza- Edwards, A., Bocanegra-García, G., Rosales-Hoz, L., de Pablo-Galán, L., 1998, Beach sands from Baja California Peninsula, México: Sedimentary Geology, 119, 263-274.

Carranza-Edwards A., Centeno-García L., Rosales-Hoz L., Lozano-Santa Cruz R., 2001, Provenance of beach gray sands from western México: Journal of South American Earth Sciences, 14, 291-301.

Dickinson, W.R., Beard, L.S, Brakenridge, G.R., Erjavec J.L., Ferguson R.C., Inman K.F., Knepp R.A., Lindberg F.A. Ryberg P.T., 1983, Provenanve of North American Phanerozoic sandstones in relation to tectonic setting: Geological Society of America Bulletin, 94, 222-235.

Dutta, P.K., Zhou, Z, dos Santos, P.R., 1993, A theoretical study of mineralogical maturation of eolian sand: Geological Society of America. Special Paper, 284, 203-209.

Fernández-Eguiarte, A., Gallegos-García, A., Zavala-Hidalgo, J., 1992, Oceanografía Física 1 (Masas de Agua y Mareas de los Mares Mexicanos), escala 1:4,000,000: México, Universidad Nacional Autónoma de México, Instituto de Geografía, Atlas Nacional de México, Tomo II, IV. Naturaleza, 9. Oceanografía, map IV.9.1.

Folk, L , 1980, Petrology of Sedimentary Rocks: Austin Texas, Hemphill, 182 p.

Floyd, P.A., Winchester, J.A., Park, R.G., 1989, Geochemistry and tectonic setting of Lewisian clastic metasediments from the Early Proterozoic Loch Maree Group of Gairloch, N.W. Scotland: Precambrian Research, 451, 203-214.

Franzinelli, E., Potter, P.E., 1983, Petrology, chemistry and texture of moder river sands Amazon River System: Journal of Geology, 91, 23-29.

Gallet, S., Jahn, B.M., Torii, M., 1996, Geochemical characterization of the Luochuan loess-paleosol sequence, China, and paleoclimatic implications: Chemical Geology, 133, 67-88.

Garzanti E., Andó S., Vezzoli G, Dell´era D., 2003, From rifted margins to foreland basin: investigating provenance and sediment dispersal across desert Arabia (Oman, U.A.E.): Journal of Sedimentary Research, 73, 572-588.

Hawkesworth, C.J., Morrison, M.A., 1978, A reduction in ^{87}Sr / ^{86}Sr during basalt alteration: Nature, 276, 381-383.

Hill, I.G., Meighan, I.G., Worden, R.H., 2000, Yttrium: the immobility-mobility transition during basaltic weathering: Geology, 28, 923-926.

Honda M., Yabuki S., Shimizu H., 2004, Geochemical and isotopic studies of aeolian sediments in China: Sedimentology, 51, 211-230.

Inman D.L., Ewing, G.C., Corliss, J.B., 1966, Coastal sand dunes of Guerrero Negro, Baja California, Mexico: Geological Society of America Bulletin, 77, 787-802.

Kasper-Zubillaga J.J., Carranza-Edwards A., Rosales-Hoz, L., 1999, Petrography and geochemistry of Holocene sands in the western Gulf of Mexico: implications for provenance and tectonic setting: Journal of Sedimentary Research, 69, 1003-1010.

Kasper-Zubillaga J.J., Carranza-Edwards A., 2005, Grain size discrimination between sands of desert and coastal dunes from northwestern Mexico: Revista Mexicana de Ciencias Geológicas, 22(3), 383-390.

Kasper-Zubillaga, J.J., Dickinson, W.W., 2001, Discriminating depositonal environments of sands from modern source terranes using modal analysis: Sedimentary Geology, 143, 149-167.

Kasper-Zubillaga, J. J., Zolezzi-Ruíz, H., Carranza-Edwards, A., Girón-García, P., Ortiz-Zamora, G., Palma, M., 2006, Sedimentological, modal analysis and geochemical studies of desert and coastal dune sands, Altar Desert, NW Mexico: Earth Surface Processes and Landforms, DOI:101002/esp1402.

Kasper-Zubillaga, J.J., Acevedo-Vargas, B., Morton-Bermea, O, Ortiz-Zamora, G., in press, Rare earth elements of the Altar Desert dune and coastal sands, Northwestern Mexico: Chemie Der Erde

Geochemistry.

Khalaf, F., 1989, Textural characteristics and genesis of the aeolian sediments in the Kuwaiti desert: Sedimentology, 36, 253-271.

Köeppen, W., 1948, Climatología: México, Fondo de Cultura Económica, 478 p.

Krupka K.M., Serne R.J., 2002, Geochemical factors affecting the behaviour of antimony, cobalt, europium, technetium and uranium in vadose sediments: U.S.A., Department of Energy, Pacific Northwest National Laboratory, 95 p.

Lancaster , N., 1983, Controls on dune morphology in the Namib Sand Sea, *in* Brookfield, M.E., Ahlbrandt, T.S. (eds.), Eolian Sediments and Processes: Amsterdam, Elsevier, 261-289.

Lancaster N., 1992, Relations between dune generations in the Gran Desierto of Mexico: Sedimentology, 39, 631-644.

Lancaster, N., 1995, Origin of the Gran Desierto Sand Sea, Sonora, Mexico: Evidence from dune morphology and sediments *in* Tchakerian V.P. (ed.). Desert Aeolian Processes: New York, Chapman and Hall, 11-36.

Livingstone I., Bullard J.E., Wiggs G.F.S., Thomas D.S.G., 1999, Grain-size variation on dunes in the Southwest Kalahari, Southern Africa: Journal of Sedimentary Research, 69, 546-552.

Lee, C.T.A. , 2002, Platinum-group element geochemistry of peridotite xenoliths from the Sierra Nevada and the Basin and range, California: Geochimica et Cosmochimica Acta, 66, 3987-4005.

Leeder, M.R., 1982, Sedimentology: Process and Product: London, Allen and Unwin, 344 pp.

Muhs, D.R., Bush, C.A., Cowherd, S.D. Mahan, S., 1995, Geomorphic and geochemical evidence for the source of sand in the Algodones dunes, Colorado desert, southeastern California, *in* Tchakerian,V. P. (ed.), Desert Aeolian Processes: London., Chapman and Hall, 37-74.

Muhs, D.R., Holliday, V.T., 2001, Origin of late Quaternary dune fields on the Southern High. Plains of Texas and New Mexico: Geological Society of America Bulletin, 113, 75-87.

Muhs, D.R., Reynolds R.L., Been J., Skipp G., 2003, Eolian sand transport pathways in the southwestern United States: importance of the Colorado River and local sources: Quaternary International, 104, 3-18.

Muhs, D.R., 2004, Mineralogical maturity in dune fields of North America, Africa and Australia: Geomorphology, 59, 247-269.

Nagarajan, R, Madhavaraju, J., Nagendra, R., Armstrong-Altrin, J.S., Moutte, J., 2007, Geochemistry of Neoproterozoic shales of the Rabanpalli Formation, Bhima Basin, Northern Karnataka, southern India: implications for provenance and paleoredox conditions: Revista Mexicana de Ciencias Geológicas, 24, 150-160.

Nesbitt, H.W., Young, G., 1982, Early Proterozoic climate and plate motions inferred from major chemistry of lutites: Nature, 279, 715-717.

Nesbitt, H.W., Young, G., 1996, Petrogenesis of sediments in the absence of chemical weathering: effects of abrasion and sorting on bulk composition and mineralogy: Sedimentology, 43, 341-358.

Padilla y Sánchez, R.J., Aceves-Quesada, J.F., 1992, Geología, escala 1:4,000,000: México, Universidad Nacional Autónoma de México, Instituto de Geografía, Atlas Nacional de México, Tomo II, IV. Naturaleza, 1. Geología, map IV.1.1.

Pérez-Villegas, G., 1989, Viento Dominante Durante el Año, escala 1:4,000,000: México, Universidad Nacional Autónoma de México, Instituto de Geografía, Atlas Nacional de México, Tomo II, IV. Naturaleza, 4. Clima, map IV.4.2.

Pye, K. , Tsoar, H., 1990, Aeolian Sand and Sand Dunes: London, Unwin Hyman, 396 pp.

Pye, K., 1991, Beach deflation and backshore dune formation following erosion under surge conditions: an example from Northwest England: Acta Mechanica, 2, 171-181.

Pye, K., Mazullo, J., 1994, Effects of tropical weathering on quartz shape: an example from northeastern Australia: Journal of Sedimentary Research, A64, 500-507.

Roser, B.P., Korsch, R.J., 1986, Determination of tectonic setting of sandstone-mudstone suites using SiO_2 content and K_2O/Na_2O ratio: The Journal of Geology, 94, 635-650.

Sawyer, E.W., 1986, The influence of source rock type, chemical weathering and sorting on the geochemistry of clastic sediments from the Quetico metasedimentary belt, Superior Province, Canada: Chemical Geology, 55, 77-95.

Sutarno, R., Steger, H.F., 1985, The use of certified reference materials in the verification of analytical data and methods: Talanta, 32, 439-445.

Tamayo, J.L., 2000, Geografía Moderna de México: México, Editorial Trillas, 512 p.

Verma, S.P., 1997, Sixteen statistical tests for outliers detection and rejection in evaluation of International Reference Materials; example of microgabbro PM-S: Geostandards Newsletters, Journal of Geostandards and Geoanalysis, 21, 59-75.

Verma, S.P, Quiroz-Ruiz, A., 2006, Critical values for 22 discordancy test variants for outliers in normal samples up to sizes 100, and applications in science and engineering: Revista Mexicana de Ciencias Geológicas, 23, 302-319.

Wang, X., Dong, Z., Zhang, J., Qu, J. Zhao, A., 2003, Grain size characteristics of dune sands in the central Taklimakan Sand Sea: Sedimentary Geology, 161, 1-14.

Watson, A., 1986, Grain-size variations on a longitudinal dune and a barchan dune: Sedimentary Geology, 10, 77-106.

Weltje, G.J., 2002, Quantitative analysis of detrital modes: statistically rigorous confidence regions in ternary diagrams and their use in sedimentary petrology: Earth Science Review, 57, 211-253.

Winspear, N.R., Pye, K., 1995, Sand supply to the Algodones dunefield, south-eastern California USA: Sedimentology, 42, 875-891.

Zimbelman, J.R., Williams, S.H., 2002, Geochemical indicators of separate sources for eolian sands in the eastern Mojave Desert California and western Arizona: Geological Society of America Bulletin 114, 490-496.

Zolezzi-Ruiz, H., 2007, Modelo Composicional de las Dunas de Bahía Sebastián Vizcaíno, México: Distribución de Tamaño de Grano, Petrografía, Geoquímica e Implicaciones de la Procedencia del Sedimento: Mexico, D.F., Universidad Nacional Autónoma de México, tesis de maestría, 180 p.

Manuscript received: May 17, 2007
Corrected manuscript received: September 7, 2007
Manuscript accepted: September 9, 2007